The 30–40 Day Oscillations Simulated in an "Aqua Planet" Model

By Yoshi-Yuki Hayashi and Akimasa Sumi

Geophysical Institute, University of Tokyo, Tokyo 113, Japan
(Manuscript received 7 February 1986, in revised form 31 May 1986)

Abstract

Numerical experiments using a general circulation model (GCM) were performed for the purpose of investigating the possibility of the generation of a long period (30–40 days) oscillation as a collective motion of cumulus activity (so-called wave-CISK) along the equator of an ocean covered globe ("aqua planet"). In our model, the SST distribution was symmetric about the equator and uniform in the longitudinal direction.

The results of a 90 day integration exhibited the spontaneous appearance of a collective motion of convective activity together with an east-west wavenumber one circulation (the "30 day oscillation"). The characteristics of this east-west circulation resemble those of the observed 30–60 day oscillation in the actual atmosphere. The 30 day oscillation is characterized by a superposition of two different scales: the scale of precipitation patterns ("super clusters") which is nearly equal to the equatorial radius of deformation, and the scale observed as the modulation of precipitation patterns and the east-west circulation with a wavenumber one. The whole structure moves eastward at a slow phase speed (15 m/s).

The results also exhibited the spontaneous formation of double ITCZs around the equator. Thus the production of the double ITCZ structure does not necessarily require a minimum SST at the equator. In the equatorial region between the north and south ITCZs, active convection forms super clusters, while in the regions poleward of the ITCZs, active convection forms tropical cyclones.

Another experiment without the moist processes resulted in the abrupt disintegration of the 30 day oscillation into Kelvin and Rossby waves. This indicates that strong mode coupling between the equatorial free waves is required in order to maintain the 30 day oscillation. The slow phase speed, the strong mode coupling and the double structure in scale indicate that the collective motion of convective activity along the equator cannot be explained simply as a Kelvin wave mode of the linear equatorial wave-CISK theory presented so far. The 30 day oscillation should be regarded as a new type solution of the equatorial wave-CISK problem.

1. Introduction

In recent years, the large scale variability known as the 30–60 day oscillation has been recognized as a dominant component of the intraseasonal variability of the equatorial circulation (*e.g.,* Madden and Julian, 1972; Yasunari, 1981; T. Murakami *et al.,* 1984; Quah, 1984; M. Murakami, 1985). It has been demonstrated that the 30–60 day oscillation plays an important role even in the interannual variability of the equatorial region. For instance, the appearance of anomalous convection in the central Pacific and drought over the maritime continent – Australia region during the ENSO (El-Niño Southern Oscillation) events is recognized as a shift in the distribution of the 30–60 day oscillation (see, Fig. 15 of Lau and Chan, 1985).

The characteristics of the 30–60 day oscillation obtained from these observational studies may be summarized as follows:

(1) Zonal wavenumber one structure is dominant especially in the zonal component of the wind field (u). (*e.g.,* Madden and Julian, 1972; Yasunari, 1981; T. Murakami *et al.,* 1984; Quah, 1984).

(2) The zonal wind (u) has a baroclinic structure (opposite sign between the lower troposphere (850 mb) and the upper troposphere

(200 mb)), and the signal is confined to the troposphere (T. Murakami and Nakazawa, 1985).

(3) The signal propagates eastward at a speed of about 10–15 m/s, which is much slower than the phase speed of the equatorial Kelvin waves with the same vertical wavelength (about 30–60 m/s with a half wavelength of 8–15 km and the buoyancy frequency of $N^2 = 10^{-4}$ s^{-2}) (e.g., Madden and Julian, 1972; Parker, 1973; Chang, 1977). The signal sometimes also appears to be of a standing nature over the eastern Indian Ocean-Western Pacific region with a node of u-wind over Indonesia (T. Murakami et al., 1984; Yamagata and Y. Hayashi, 1985).

(4) There is a phase tilt of coherence in the north-south direction (Madden and Julian, 1972; T. Murakami and Nakazawa, 1985). Both u-wind (Yasunari, 1981) and outgoing long wave radiation (OLR) (M. Murakami, 1984) seem to propagate northward.

(5) The signal in OLR is stronger over the ocean than over the land (Fig. 1 of T. Murakami et al., 1986; Fig. 1 of Knutson et al., 1986).

Compared with recent advances in observational studies as summarized above, investigations into the origin and mechanism of the 30–60 day oscillation seem to be still in the preliminary stage. The efforts made so far in theoretical and simulation studies are summarized as

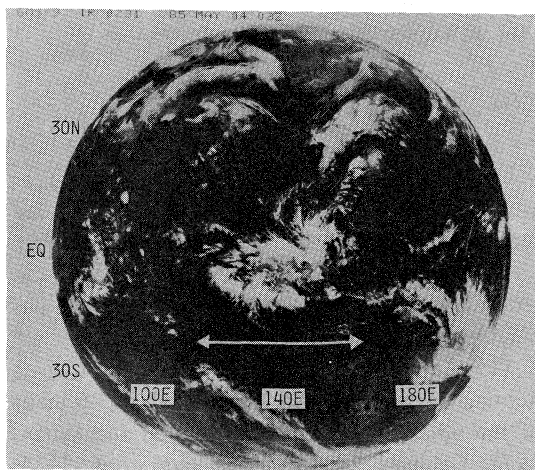(1) modifying equatorial wave dynamics

Fig. 1   IR imagery taken from the GMS on May 4, 1985 (from Monthly Report of Meteorological Satellite Center, May 1985). A super cluster (denoted by an arrow) appears over the maritime continent.

(especially, equatorial Kelvin waves) (e.g., Chang, 1977).

(2) considering the role of land-sea contrast and moisture distribution (e.g., Webster, 1983),

(3) looking for an oscillation of the zonally symmetric circulation with an intraseasonal time scale by the use of a zonally symmetric general circulation model (Goswami and Shukla, 1984).

A difficulty in interpreting the 30–60 day oscillation as an equatorial Kelvin wave is the large difference between the phase speed of free waves (30–60 m/s) and the observed eastward propagation speed (10–15 m/s). Chang (1977) introduced a dissipation with a time constant of about 5 days, and found a frictional mode with a reduced phase speed for a given set of zonal and vertical wavelengths. He showed that the amplitude is maximum for the largest horizontal scale when the forcing (cumulus heating) has a fixed amplitude regardless of wavenumber. However, it has not yet been shown how the particular heating distribution can be realized, and how the wave structure could be maintained against the dissipation.

Webster (1983) considered the effect of the land-sea contrast (differential heating of land and ocean due to the surface moisture condition), and showed that the northward propagation of the signal can occur over the Indian ocean. However, the 30–60 day signal is also prominent over the western Pacific where no large land mass exists. During the 82–83 ENSO event the oscillation was observed in the active convection region located in the central Pacific. On the other hand, as compared to the western Pacific, the signal is not so apparent over the Caribbean Sea and the Gulf of Guinea where the land-sea contrast might be a possible mechanism. These facts suggest that the existence of land is not an essential factor for the 30–60 day oscillation.

The model with zonally averaged variables shows the possibility of an oscillation on the intraseasonal time scale occurring in the moist symmetric Hadley circulation (Goswami and Shukla, 1984). For the purpose of revealing the mechanism of the 30–60 day oscillation, however, consideration of the zonally symmetric oscillation is insufficient, since the zonally asymmetric (wavenumber one) structure char-

acterizes the 30–60 day oscillation.

Here, we emphasize observational fact (5): the activity of the 30–60 day oscillation is high over the ocean, especially over the oceanic regions with high SST*. In these regions the convective activity is also strong (low OLR) even in the mean state. During the 82–83 ENSO event, the warm SST region expanded eastward and the region of the strong 30–60 day signal of OLR also expanded eastward (Lau and Chan, 1985). Sardeshmukh and Hoskins (1985) also demonstrated that during the 82–83 event the 200 mb vorticity activity of the 30–60 day time scale is very strong over the central Pacific around the east of the date line.

From this observational fact we can speculate that the 30–60 day oscillation occurs as an intrinsic property of an interactive system of large-scale flow and equatorial convection over the ocean with a sufficiently large area of high-SST (such as the western Pacific, the eastern Indian Ocean, or the mid-Pacific during the ENSO events). When the area of high-SST ocean is large enough, an oscillation of convective activity is caused. An OLR anomaly with a spatial extent of the order of 3000 km (Lau and Chan, 1983a, b; M. Murakami, 1984; Knutson et al., 1985) might manifest such an oscillation. Fig. 1 (IR** imagery) shows a typical example of cloud activity lying over the maritime continent. The region of active convection denoted by an arrow in Fig. 1 is composed of a group of so-called cloud clusters, and thus it can be referred to as a "super cluster" on a scale of 3000 km. By observing sequential IR imageries, the 30–60 day oscillation can be recognized as a motion of these super clusters.

The behavior of these anomalies suggests that convective activity cannot be equally distributed over a large region exteding from the Indian Ocean to the western Pacific at one time. When the convection is active over the Indian Ocean, the activity over the western Pacific is suppressed, and vice versa; even if the SST is almost equally high in both regions.

Going a step further, we expect that the idealistic 30–60 day oscillation would be real-

ized if the entire surface of the globe is covered with a zonally uniform ocean. On such a uniform boundary, cumulus convection at the equator would occur collectively within an areal extent of about 3000 km (super clusters) and move eastward coherently. The idealistic form of the 30–60 day oscillation can be described mathematically as a symmetry breaking where an asymmetric distribution of cumulus activity takes place in spite of the symmetric (zonnaly uniform) surface conditions.

In the following sections we present the results of numerical experiments using a general circulation model (GCM). Here, our purpose is to investigate the idealistic behavior of convective activity and associated large scale motions over a zonally uniform area of potentially active moist convection. The whole surface is covered with ocean ("aqua planet"). The SST distribution is zonally uniform and symmetric about the equator, and hence, the potential for the occurrence of moist convection is equal in the longitudinal direction. The main conclusion is that, in spite of the zonally symmetric surface conditions, small scale patterns (<3000 km) appear in the precipitation field and the wavenumber one structure appear in the circulation field. The whole structure propagates eastward at a phase speed of 15 m/s (a period of 30 days for wavenumber one). The simulated signal is, hereafter, referred to as the "30 day oscillation". The mechanism of the 30 day oscillation is discussed in Section 4 as a modification of the equatorial wave-CISK theory. Detailed analysis to reveal the model dynamics is now underway at the University of Tokyo.

2. Model and experimental design

The general circulation model used here is basically the operational weather prediction model of the Japan Meteorological Agency, which was originally designed by Kanamitsu et al. (1983) and updated by N. Sato. It is a global spectral model with a 42 wave triangular truncation and 12 vertical levels. The performance and systematic errors of the original model are given in Kanamitsu et al. (1983) and Sumi and Kanamitsu (1984) for its hemispheric version.
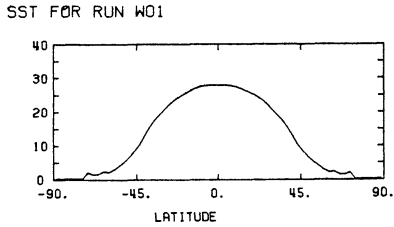
---

*sea surface temperature
**infrared

Fig. 2 Zonal profile of the SST distribution employed in the simulation.

2.1 The surface conditions

The whole globe is covered with an ocean whose SST distribution is uniform in the zonal direction and symmetrical about the equator. The model SST (Fig. 2) was derived from averaging the April climatic temperature of all the oceans longitudinally and from taking the mean of the Northern and the Southern Hemisphere distribution. The model SST is fixed (not predicted), and affects the atmospheric temperature and water vapor content through boundary fluxes. The fluxes from the sea surface are given by the bulk formula.

2.2 Radiation (shortwave)

The position of the sun (solar declination) was fixed at equinox, but the diurnal variation included in the original model was not changed. The absorption of O_3 is given by the two-hemispheric and zonal average of the climatological value of April. The absorption due to H_2O and scattering due to clouds are calculated through the predicted amount of water vapor.

2.3 Cumulus parameterization

The parameterization scheme developed by Kuo (1974) is used in the model. The criteria for adjustment are

(1) conditionally unstable stratification,

(2) convergence of moisture flux in the cloud layer,

(3) mean relative humidity in the cloud layer greater than the critical value (90%).

Here the cloud layer is defined as the layer between the cloud base (the first level above the planetary boundary layer where the stratification is conditionally unstable) and the cloud top where the moist adiabat intersects the environmental temperature of the model.

2.4 Initial conditions and time integration

Two experiments were carried out. The "wet" experiment was started from the initial value derived from taking the zonal and two-hemispheric average of the monthly mean grid data of April 1979 produced by ECMWF. The model was integrated for 90 days and the results are shown in Figs. 3–6. The "dry" experiment was started from $t = 45$ days of the first experiment, but with the water processes excluded (dry atmosphere). The model was integrated for 55 days (Fig. 7).

3. Results

3.1 Signal of the about 30 day period

Fig. 3a shows the time-longitude section of the zonal wind deviation u' at the 850 mb level at the equator. (The definition of symbols is summarized in the Appendix.) Note that in the longitudinal direction the diagram is duplicated to clarify the periodicity of the signal. The time interval for data sampling is 24 hours (once a day). No time-space filtering technique was utilized in obtaining Fig. 3. It is evident from the figure that a clear zonal wavenumber one structure (a pair of easterly and westerly) emerges spontaneously after about 20 days. The structure propagates eastward at a speed of about 15 m/s (period of about 30 days).

It is surprising that the signal is quite regular in the zonal wind at the equator. The term, "30 day oscillation", is used here to distinguish the signal obtained in this aqua planet model from the 30–60 day oscillation in the actual atmosphere. The structure of the "30 day oscillation" resembles the observed 30–60 day oscillation as will be presented later; the term "oscillation" is retained, even though it would seem more appropriate to call it a wave.

The time-longitude section of the 12 hour integrated precipitation is shown in Fig. 3b. In contrast with the wind pattern, small scale structures dominate the distribution of precipitation (cf. Fig. 4). The sampling rate is doubled for Fig. 3b (twice a day) in order to resolve the motion of these small scale structures. It should be noted that the largest scale of precipitation patterns is less than 3000 km. As will be explained in the next subsection, we
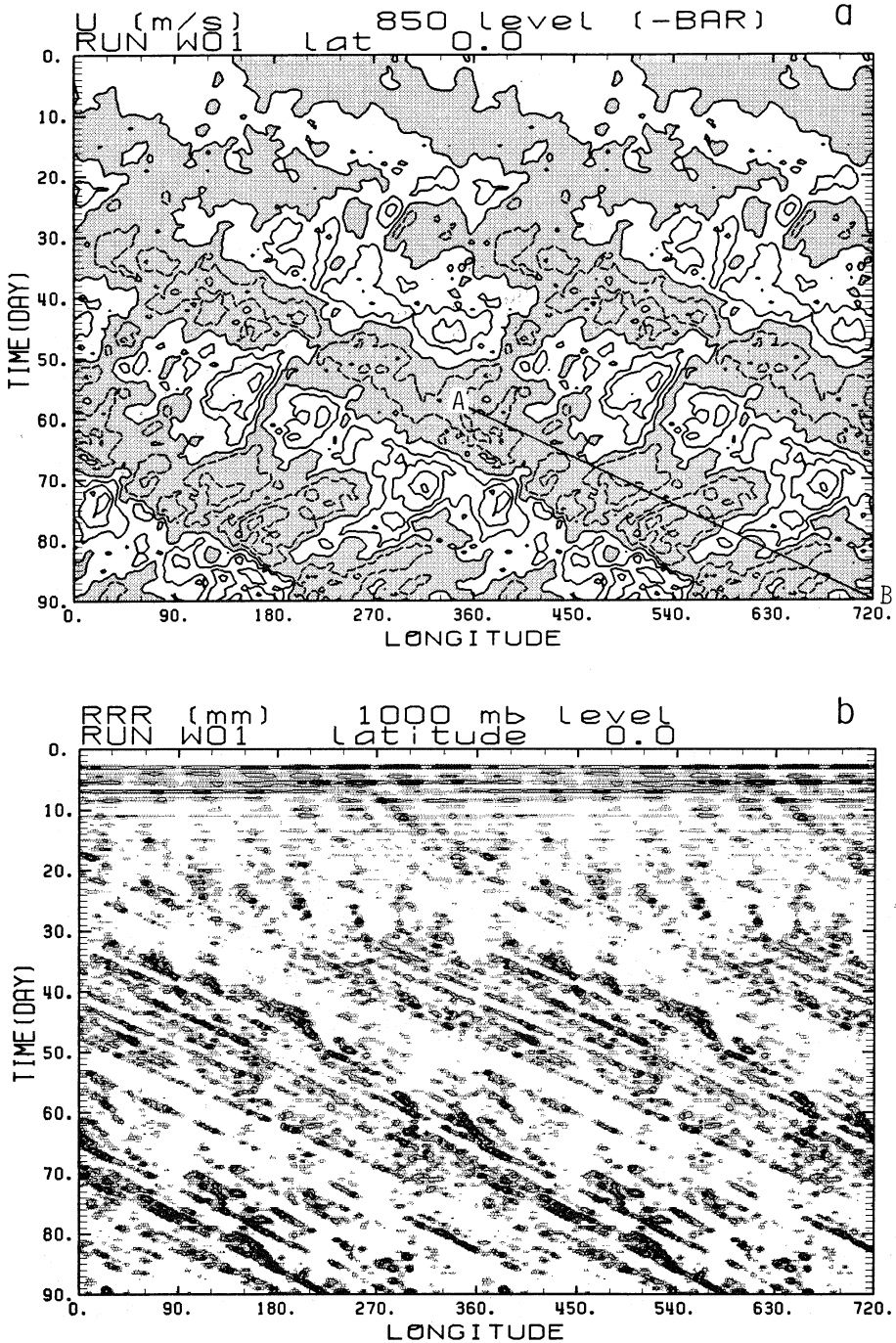
Fig. 3   Longitude-time sections of (a) 850 mb zonal wind deviation (u') and (b) precipitation per 12 hours. The figures are duplicated in the longitudinal direction to clarify the periodicity. The contour intervals are 2.5 m/s for u' and 2.5 mm/12 h for precipitation. The regions of (a) easterly ($u' < 0$) and (b) precipitation greater than 1 mm/12 h are shaded. The line segment AB denotes the phase line (c_0 = 15 m/s) along which the composite structures are constructed.

consider these small patches of precipitation pattern to correspond to the "super clusters" often seen in the IR satellite imageries especially over the western Pacific (Fig. 1). The dominance of small scale structures appears also in ω' and the horizontal divergence fields (not shown). In Fig. 3b the precipitation patches move coherently along the phase line of 15 m/s. A comparison between Figs. 3a and 3b indicates that these small structures are modulated by wavenumber one. Intense precipitation tends to occur near the longitude where the westerly changes to the easterly.

The successive formation of precipitation along the phase line as shown in Fig. 3b cannot be observed poleward of 12° (not shown). The precipitation patches of these latitudes are usually due to disturbances which are considered to be tropical cyclones (as will be explained later), and they do not move systematically in the longitudinal direction.

3.2 Horizontal structure

Snap shots of the horizontal distribution of precipitation are shown in Fig. 4. The four figures correspond to the time $t = 66, 74, 82, 90$ days. There appear three types of precipitation patterns. In the mid-latitudes, band structures oriented in the north-south direction caused by baroclinic waves can be seen. In the latitudes between 10° and 30°, circular areas of intense precipitation are observed; these are associated with vorticity and low surface pressure (not shown), and hence considered to be tropical cyclones. Around the equator (between 10N and 10S), precipitation patches on the scale of about 3000 km can be seen. These correspond to the eastward propagating precipitation areas shown in Fig. 3b. They are not associated with strong vorticity like that of tropical cyclones. It is not difficult to recognize in Fig. 4 that the distribution of these precipitation patches is modulated, producing the wavenumber one structure, and
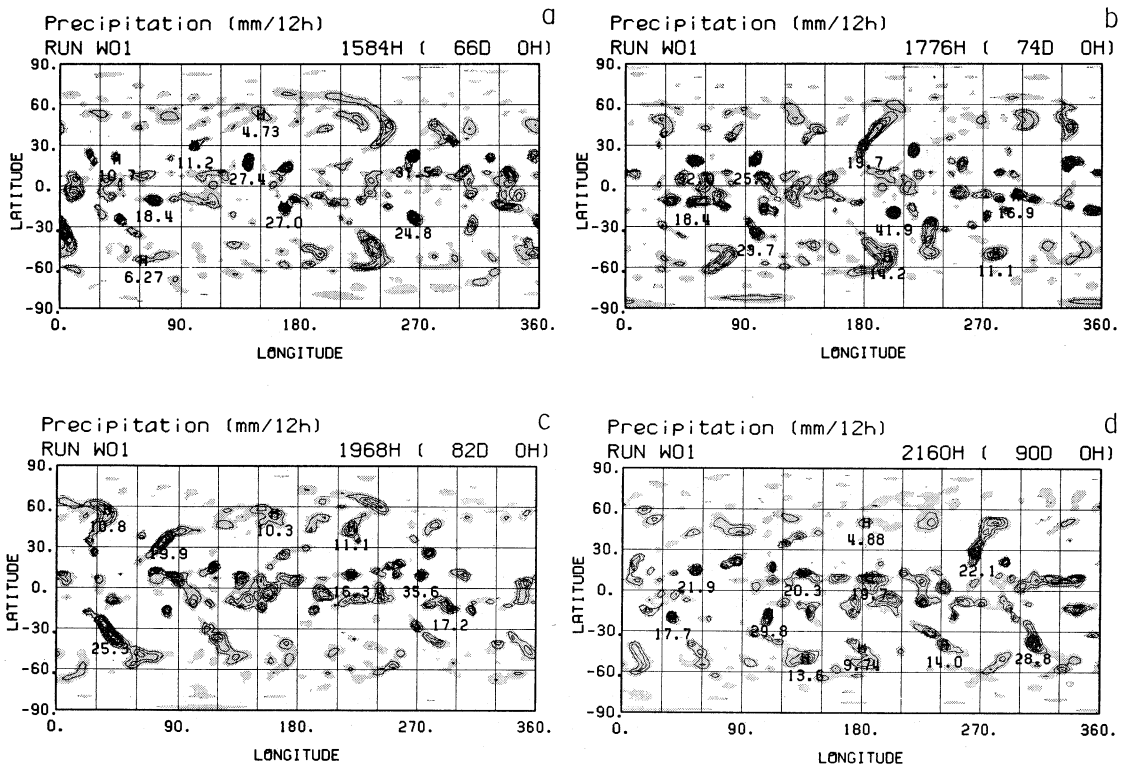

Fig. 4   Snapshots of precipitation per 12 hours at four different times ($t = 66, 74, 82, 90$ days). The contour interval is 2.5 mm/12 h and the regions of precipitation greater than 1 mm/12 h are shaded.

are moving to the east. On the 66th day, most of the precipitation areas are concentrated in the region between the longitudes 270° and 30°. They then move gradually eastward and are found between 0° and 120° on the 74th day, between 90° and 210° on the 82nd day, and between 180° and 300° on the 90th day.

We emphasize here that the precipitation patches appearing in Fig. 4 are not far from the convection features of the real atmosphere. The scale of these precipitation patches at the equator corresponds to that of super clusters observed in IR imageries (Fig. 1) and of OLR anomalies in, for example, Lau and Chan (1983a, b) and Weickmann et al. (1985). The period of intense precipitation at a fixed longitudinal point is about 2 to 4 days (Fig. 3b) except for the dry phase (e.g., around t = 50 days at the longitude

360°) of the 30 day oscillation. The existence of the time scale of 2 to 4 days in the precipitation field was reported by M. Murakami (1972). He showed that disturbances of this time scale move eastward, and that they are not associated with intense vorticity. These characters resemble those of the precipitation patches obtained in the model. Recently, Nakazawa (1986) produced an interesting figure on the motion of super clusters at the equator. His time-longitude section of negative OLR anomalies is quite similar to Fig. 3b.

Since our model cannot resolve individual cloud clusters, only the large scale structures are reproduced as a continuous area of precipitation with the same size (<3000 km). In the model there are many (~10) super clusters along the equator, in contrast to the real situa-
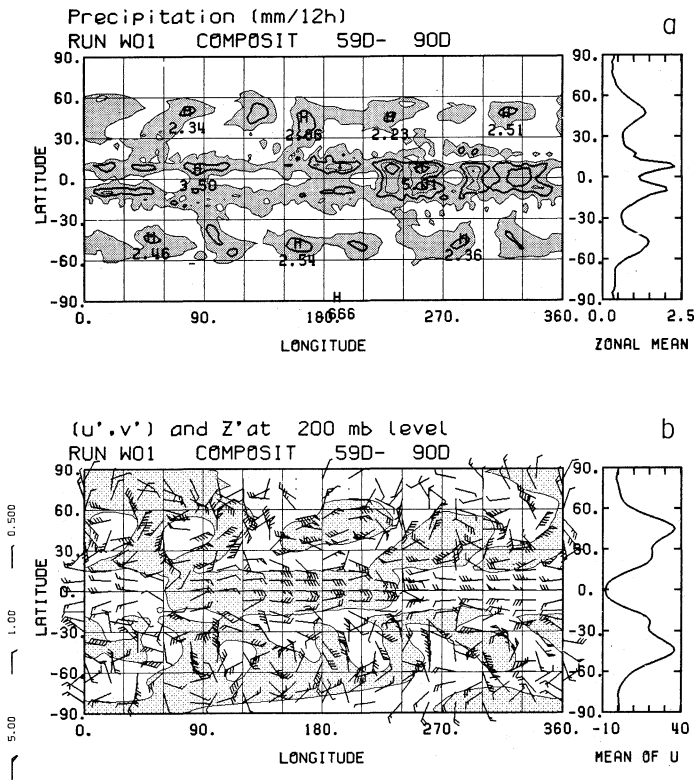

Fig. 5 Composite fields along the phase speed c_0 = 15 m/s for t = 59–90 days of (a) precipitation and (b) wind deviation (u', v') and geopotential height (Z') at 200 mb. The regions of (a) precipitation greater than 1 mm/12 h and (b) Z' < 0 are shaded. The contour interval for (a) is 1 mm/12 h. The unit of barbs plotted to the left is m/s. Zonal mean values of (a) precipitation (mm/h) and (b) zonal wind (m/s) are plotted to the right side of each figures.

tion where usually only one or two super clusters are found over the Indian Ocean or over the western Pacific. The cause of this discrepancy may be attributed to the distribution of SST. Namely, the highest SST exists all along the equator in the model, while in the real situation the highest SST region is limited to the Indian Ocean-western Pacific region.

An important point in regard to super clusters is that, even under zonally symmetric surface conditions, the convective activity cannot cover regions larger than about 3000 km at one time. Note that because of the model truncation (the largest wavenumber is 42), the smallest precipitation patches appearing in the model correspond to almost the shortest resolvable wavelength at the equator (=1000 km). Thus, their individual character may be affected by the model truncation. Nevertheless, the model resolution seems adequate for describing the larger scale ($\sim$3000 km) convective activity.
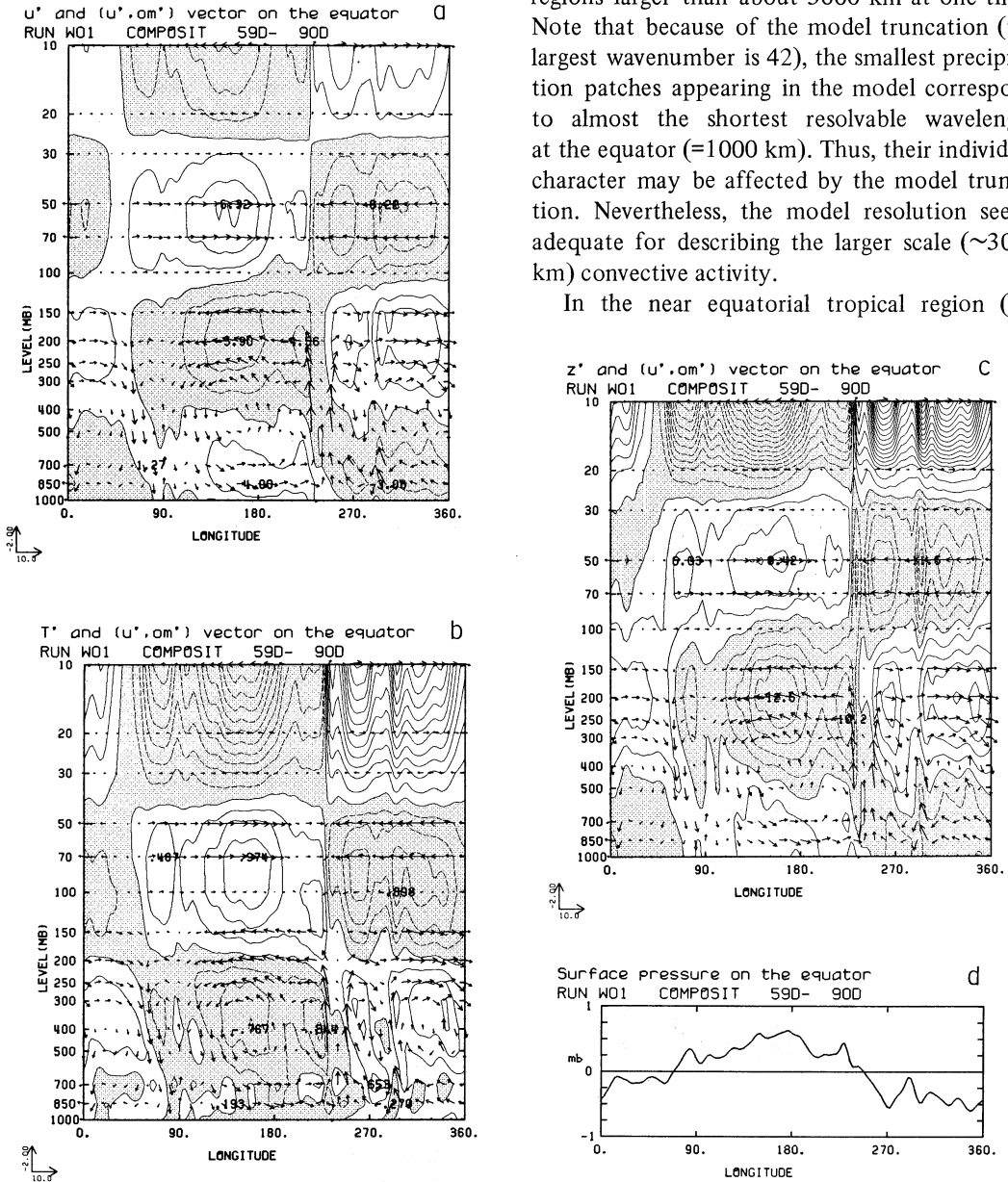
In the near equatorial tropical region (be-

Fig. 6 Vertical cross sections of composite fields on the equator along the phase speed c_0 = 15 m/s for t = 59–90 days of (a) zonal wind deviation u' (m/s), (b) temperature deviation T' (K) (c) height deviation Z' (m) and (d) surface pressure deviation P_S' (mb). The contour intervals are 2.0 m/s for u', 0.25 K for T' and 2.5 m for Z'. The vectors indicate (u', ω'). The unit for vectors is (m/s, mb/hour).

tween 10N and 10S), there are bands of strong precipitation. The zonal and time ($t = 59$–90 days) mean value of the precipitation is plotted along the right side of Fig. 5a which shows a double ITCZ structure around the equator. Corresponding to this precipitation feature, the zonal mean vertical wind (not shown) is upward at 10N and 10S, but it is downward at the equator. To the north or south of the ITCZs, the modulation due to wavenumber one is not recognized. Tropical cyclones seem to appear in rather a random manner, although there remains the possibility of some modulation which can be detected only through statistical procedure.

The interesting point of the double ITCZs is that the aqua planet model produces double ITCZs even when SST minimum does not exist above the equator. Pike (1971) indicated the existence of double ITCZs by employing a zonally symmetric air-sea coupled model. But in his study it was necessary to have low SST at the equator caused by equatorial upwelling. Our result (Fig. 5a), contrary to that of Pike, seems to support the idea that double ITCZs are caused where Ekman convergence is large enough (Charney, 1971).

To reveal the structure associated with the 30 day oscillation, composites of variables along the phase speed $c_0 = 15$ m/s (along the line A–B of Fig. 3a) are constructed for the period of $t = 59$–90 days. The composite precipitation is shown in Fig. 5a. The zonal mean value is also plotted on the right side. In Fig. 5b, the composite structures of the 200 mb wind (u', v') and geopotential height deviation Z' are shown. Over the equator the zonal wind u' at the 200 mb level is in the opposite direction to that of the 850 mb level (cf. Fig. 6). The latitudinal extent of the signal in u' is 1000–1500 km which is close to the equatorial radius of deformation: $\sqrt{c/\beta} = 1500$ km where $c = 50$ m/s is the phase speed of the internal wave mode with roughly the same vertical wavelength as obtained in the model (see Fig. 6). The values of 6 m/s for u' and 13 m for Z' (cf. Fig. 5) satisfy the geostrophic balance relationship in the neighbourhood of the equator ($\beta u' = -d_{yy} gZ'$) by assuming the characteristic latitudinal scale of about 1000 km.

By comparing Fig. 5a with Fig. 5b, it is clear that the most intense convection in equatorial latitudes occurs at the boundary of the easterlies and westerlies. Precipitation activity is spread over the westerly region at 200 mb (to the east of the strongest convection) at the equator, while at the ITCZ latitudes (10N and 10S) there is a tendency for fairly strong convections to occur even to the west of the strong convection.

The modulation due to the zonal wavenumber one is very effective at the equator. At higher latitudes, the formation of tropical cyclones observed as intense precipitation patches in Fig. 4 seems to obscure the structure.

3.3   Vertical structure

Composite longitude-height cross sections are presented in Fig. 6. As mentioned already in relation to the horizontal structure, the zonal wind u' (Fig. 6a) exhibits a clear baroclinic structure with different signs between the lower troposphere and the upper troposphere. The half wavelength is about 12 km. The signal above the tropopause ($\sim$100 mb) may be affected by the top boundary and the low vertical resolution: there are only two σ-levels ($\sigma = 0.075$, 0.0225) in the stratosphere. It might be plausible that the 30 day oscillation in the troposphere excites wavenumber one stratospheric Kelvin waves as discovered by Wallace and Kousky (1968). Spectral analysis methods as used by Y. Hayashi and Golder (1979) may be useful for detecting such waves. They reported the existence of Kelvin waves with a period of about 15 days in their all ocean surface model. But the relation between the Kelvin waves in the stratosphere and the 30–60 day oscillation in the troposphere has not been considered yet.

In Fig. 6d, the composite profile of surface pressure along the equator is plotted (the zonal mean is subtracted). The relationship between the circulation cell and the surface pressure obtained here resembles Fig. 16A of Madden and Julian (1972). The westward phase tilt reported by T. Murakami and Nakazawa (1985) also appears in Fig. 6, which makes it possible that the energy generated by the cumulus heating is converted into the large scale motions of the
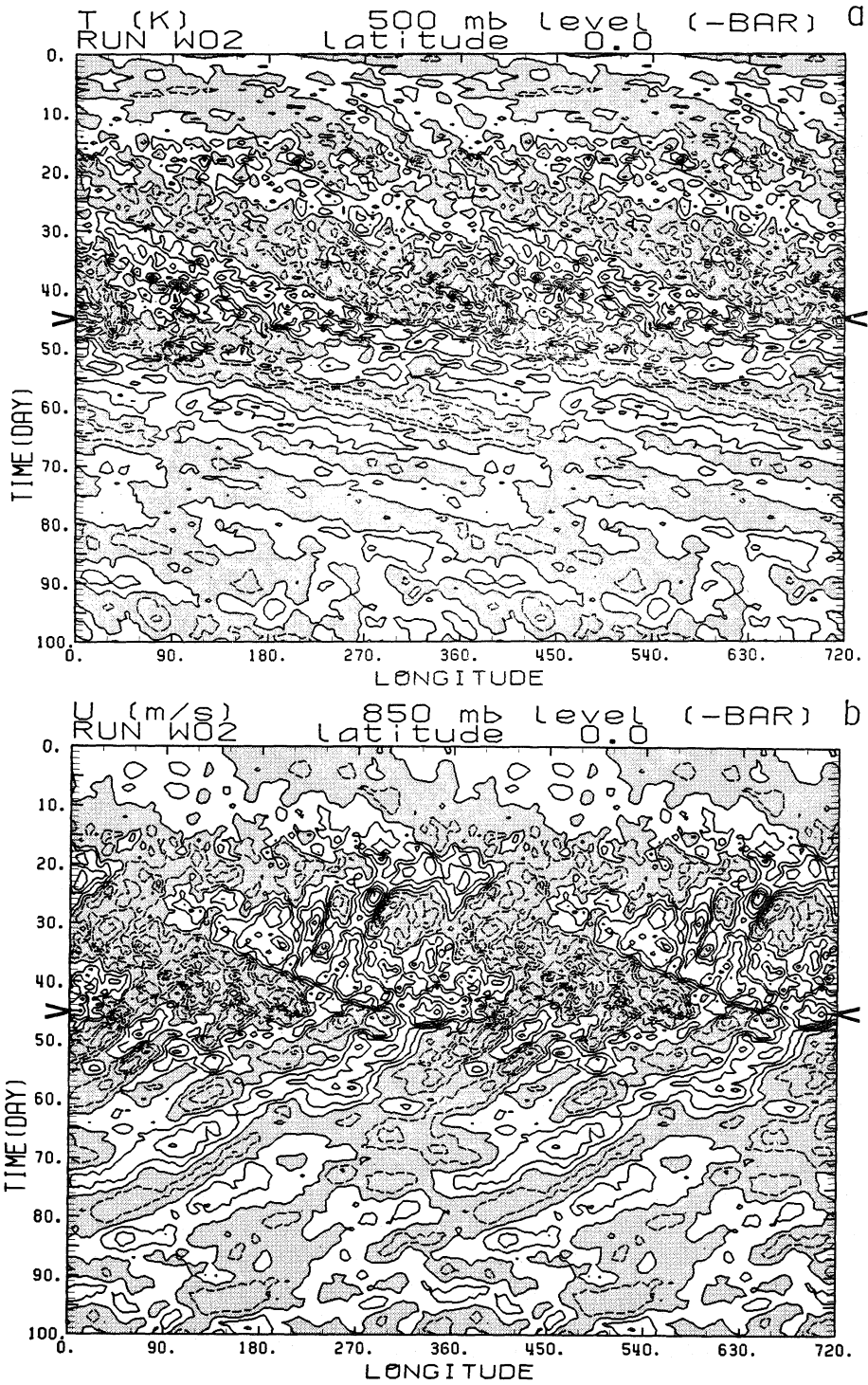
Fig. 7 Longitude-time section of (a) 500 mb T' and (b) 850 mb u' for the dry simulation. The moist processes are switched off at $t = 45$ days (cf. Fig. 3) (denoted by > <).

wavenumber one structure as described in the linear wave-CISK theory (Emanuel, 1983).

The wavenumber one structure exemplified in the composite figures (Figs. 5 and 6) exhibits characteristics similar to those of equatorial Kelvin waves (Matsuno, 1966; Gill, 1980). The upward motion (and cooling) lags behind the temperature deviation (Fig. 6b) by $\pi/2$ while the zonal wind deviation (Fig. 6a) is geostrophically balanced with the geopotential field (Fig. 6c), which in turn is hydrostatically balanced with the temperature deviation. Thus, the 30 day oscillation could be explained by some modification of linear Kelvin wave dynamics (e.g., Chang, 1977). However, as will be shown in the next subsection, the Rossby wave components are also included in the composite structure.

3.4   Dry experiment

In order to reveal the role of the moist convection in maintaining the 30 day oscillation, an experiment where the moist processes were switched off at a certain time was carried out (dry experiment). If the mechanism of the 30 day oscillation is explained by a slight modification of the dynamics of linear equatorial Kelvin waves, it would be expected that after the moist processes are removed, the structure developed would move eastward at a speed of free Kelvin waves.

The dry experiment was started from $t = 45$ days of the former run (wet experiment) but with the moist processes excluded. The dry model was integrated for 55 days. The results are presented in Fig. 7a for the time-longitude section of the 500 mb temperature (T') at the equator and in Fig. 7b for the 850 mb zonal wind (u') where the sampling rate is once a day. In Fig. 7a the time mean of T' is subtracted to eliminate the tidal signal.

The experiment resulted in an abrupt destruction of the 30 day oscillation, and the generation of free Kelvin waves propagating to the east and free Rossby waves to the west. Fig. 7a exhibits a fast signal propagating eastward at a speed of about 30–40 m/s. The vertical structure (not shown) also changes immediately: the vertical wavelength becomes about 20 km at $t = 55$ days which is a little shorter than that of the 30 day oscillation. Hence, the phase speed of 30–40 m/s is consistent with the equatorial linear dynamics (Kelvin waves). In Fig. 7b, on the other hand, a westward propagating signal is apparent. The phase speed of Fig. 7b is about one third of the eastward speed of Fig. 7a, which means that the westward disturbances are equatorial Rossby waves (Gill, 1980).

There must be vertical dispersions of Kelvin and Rossby waves. Actually, in the early period after the switching off, eastward and westward propagating signals with a small longitudinal scale seem to exist in Fig. 7. But they disappear with the passage of time. According to the dispersion relation of the equatorial modes, waves with a smaller longitudinal scale propagate upward more easily for a given vertical wavenumber. The disappearance of short waves is considered to be the result of the vertical propagation.

From Fig. 7 it can be concluded that the existence of moist processes is essential for maintaining the 30 day oscillation and the structure is composed both of equatorial free Kelvin and free Rossby waves. The moist processes cause a mode coupling between the two. The temperature field of the coupled disturbance is mostly the contribution of Kelvin waves, while the wind fluctuation comes mainly from Rossby waves.

4.   Discussion

In this section, we will discuss the mechanism of maintaining the "30 day oscillation" exhibited in the aqua planet model.

4.1   The 30 day oscillation as a wave-CISK mode

Convective activity acts as a crucial element in maintaining the 30 day oscillation; therefore, the structure realized in the model should be recognized as a new type solution of the equatorial wave-CISK problem. There is a possibility that the large scale coherent circulations which are interactively maintained by cumulus activity exist. The meaning of "new type" is that the 30 day oscillation has the following characteristics, which are not expected by the simple theories of wave-CISK presented so far (e.g., Y. Hayashi, 1970; Lindzen, 1974).

(1) Super clusters with a scale of 1500–3000 km dominate the precipitation, divergence and ω fields; and they propagate coherently eastward at a phase speed of 15 m/s.

(2) The wavenumber one (largest longitudinal scale) structure dominates the u', T' and ϕ' fields, and they also propagate eastward at a phase speed of 15 m/s. The wavenumber one structure also appears in the precipitation, divergence and ω fields as a modulating pattern of super clusters.

(3) The whole structure is composed of both equatorial free Kelvin and Rossby wave modes.

The strong mode coupling (item (3)) is not expected by the usual linear wave-CISK theory (Y. Hayashi, 1970; Lindzen, 1974). The structures of the equatorial linear wave-CISK modes obtained in these earlier works are almost equal to those of the corresponding free wave modes in the dry atmosphere, and hence the phase speed of the Kelvin wave mode which propagates eastward is two or three times as large as that of the 30 day oscillation (15 m/s). We have to alter the conventional linear wave-CISK theory to give such a slow phase speed.

Items (1) and (2) indicate that the 30 day oscillation has a double structure. There are two characteristic scales which are relevant to the equatorial wave-CISK: the equatorial radius of deformation ($\sim$1500 km) and the length of the equatorial circumference ($\sim$40000 km). The appearance of small scale structure is relevant to the classical wave-CISK theory, while the appearance of wavenumber one is caused by the finiteness of the earth. The later scale has not been considered in the earlier framework of the wave-CISK theory.

In the following subsections, the mechanism of the 30 day oscillation will be discussed separately according to the two scales mentioned above.

4.2 The existence of the super clusters

With the appearance of the small scale structures ($<$3000 km), the important point is that there exists a limit to the size of precipitation areas, and it is roughly of the order of the equatorial radius of deformation. If you would recall the zonally uniform surface conditions of our aqua planet, you would then expect that a zonally uniform precipitation pattern might result. However, the model produced precipitation patches which correspond to the super clusters in the actual atmosphere (Fig. 1). Even in the real atmosphere convection does not spread over the whole highest SST, but is more or less concentrated in the form of super clusters. Furthermore, it is puzzling why both in the model and the real atmosphere, super clusters should move eastward.

The dominance of "small" scale structures is close to the expectation of the linear wave-CISK theory. In the usual framework of the theory, the gravity modes (including the Kelvin wave mode) with shorter wavelengths have the larger growth rates, while the rotational modes have moderate growth rates (e-folding time of about 15 days). Thus, the super clusters obtained in the model seem to correspond to Kelvin or gravity modes. Note, however, that the "small" scale features appearing in the model are roughly of the order of the equatorial radius of deformation and not the shortest length resolvable in the model.

As the distance increases from the equator, the rotational (usual) CISK mechanism which acts through Ekman convergence becomes important. The feedback is unstable because heating occurs in the low-pressure region. Since the Ekman convergence is proportional to vorticity, the Rossby wave modes, which are accompanied with large vorticity, have the advantage over the gravity wave modes. The high activity of the CISK mode off the equator explains the double ITCZ structure, and in the poleward regions of the ITCZ, the CISK mechanism causes the occasional appearance of tropical cyclones.

The scale of the precipitation areas ($<$3000 km) can then be explained by the efficiency of the rotational CISK mechanism. It is most efficient for a vorticity with a scale equivalent to the radius of deformation, since there would be a balance between the efficiencies of trapping heat and the moisture supply through the Ekman pumping (Emanuel, 1983). Away from the equator the rotational CISK mechanism forms tropical cyclones with a scale of 500–1000 km. The equator is a singular point for the rotational CISK mechanism because the effect of the earth's rotation disappears there. How-

ever, through the co-existence of Ekman convergence and wave convergence, a coupling between Kelvin and Rossby modes is created, which in turns produces a structure that propagates coherently eastward. The existence of super clusters at the equator corresponds to the existence of tropical cyclones away from the equator. The rotational CISK mechanism associated with the Rossby wave component seems to be responsible for limiting the maximum size of the super clusters, while the wave-CISK (wave convergence CISK) mechanism seems to be responsible for eastward propagation. Evidence of the co-existence of the equatorial Kelvin and Rossby waves is seen in Fig. 7 where small scale eastward and westward waves appear in the T' and u' fields for a brief period just after switching off the moist processes. We shall call this particular mode "coupled Kelvin-Rossby mode" or simply KR mode.

The slow phase velocity (15 m/s) of this KR mode can be understood as the natural consequence of the mode coupling. Recent studies on the eastward propagation of the ENSO disturbances showed that the coupling between oceanic Kelvin and Rossby waves through the existence of wind stress causes a slow eastward phase speed (Philander *et al.,* 1984; Yamagata, 1985; Anderson and McCreary, 1985). For the 30 day oscillation, the moist processes play the same role as the wind stress for the ENSO disturbances.

The slow phase speed can also be understood within the linear framework by introducing a reduced gravity effect due to convection heating (Gill, 1982). Since the intense precipitations at the equator occur in the regions of upward motion (Fig. 6), the cumulus heatings reduce the adiabatic cooling, which is equivalent to reducing the static stability of the linear wave dynamics. Thereby, the eastward propagation is reduced to a certain extent when compared to the phase speed of the equatorial free Kelvin waves. It is puzzling why the linear wave-CISK theory presented so far did not obtain a considerably reduced phase speed. There is a possibility that the heating used there is too weak for reducing the adiabatic cooling. Note, here, that the effect of reduced gravity is not caused symmetrically. Cumulus heating occurs mainly

in the updraft regions and adiabatic cooling is reduced, while in the downdraft regions only adiabatic heating is active. In order to adjust the adiabatic heating to the rate of slow phase propagation, mode coupling is essential.

4.3   The effect of the finiteness of the equatorial circumference

In the previous subsection, it was emphasized that the small scale structure should be regarded as a wave-CISK mode (KR mode). In this subsection, it will be shown that the appearance of the wavenumber one can be understood as the modulation of the small-scale KR mode disturbances due to the finiteness of the equatorial circumference.

To begin with, we would like to point out that, while moist convection is usually considered to be a small scale phenomenon, it is not so small if considered together with the associated circulation. In a two-dimensional non-rotating fluid, steady circulation caused by a δ-function heating has an infinite extent in the horizontal direction (Emanuel, 1983). Since the u'-field is given as an integral quantity of the convergence, the δ-function heating (convergence) causes a circulation with the shape of a step function.

At the equator, because of the equatorial β-effect, the circulations excited by heating are confined to the equatorial radius of deformation in the latitudinal direction (the equatorial duct). These circulations ought to have a two dimensional nature: namely, they tend to extend in the longitudinal direction along the equator without any difficulty (Heckley and Gill, 1984). However, since the equatorial circulation is periodic in the longitudinal direction, the steady circulation of an infinite two dimensional flow cannot be realized. Thus, it is necessary to have a downdraft at a certain longitude along the equator.

If the KR mode has exactly the same amplitude in the zonal direction, the downdraft caused by each convective activity would have no cumulative effect. However, in the event there is a slight enhancement of convective activity somewhere along the equator, a strong downdraft region may appear on the opposite side of the equator. The appearance of asymmetry (nonuniform convective activity) has a positive feed-

back effect. The equatorial area is separated into a region where convective activity is intense, and a region where it is suppressed because of the downdraft caused by the convectively active region. The intensity of the downdraft is comparable to that of the updraft of convectively active region because the circulation is two dimensional, and hence, it is considered large enough to suppress the activity of the other region. Thus, the wavenumber one modulation of cumulus activity appears to be related to the equatorial circumference and the u'-field has the wavenumber one structure because the u'-field corresponds to the zonal average of the vertical motion field.

Following the assumption that the wavenumber one modulation is related to the equatorial circumference, the time scale of about a 10–20 days for the build up of the 30 day oscillation (Fig. 3) can be understood in the following way. If we adopt $c = 40$ m/s as a signal velocity to carry the effect of enhanced convection from one place to other place (Fig. 7), it takes about 10 days for the signal to travel around the equatorial circumference. The time for building up the 30 day oscillation is given by the time needed to establish the downdraft region on the opposite side of the equator from the convectively active region.

5. Conclusion

A GCM simulation of an atmosphere on a planet covered with zonally symmetric SST ("aqua planet") shows that an equatorial circulation system with the character of the so-called 30–60 day oscillation appears spontaneously. The characteristics of the "30 day oscillation" simulated in the model are summarized as follows:

(1) Small scale (<3000 km) structures which are regarded as the super clusters (Fig. 1) appear in the precipitation patterns. They propagate coherently eastward at a phase speed of 15 m/s.

(2) The wavenumber one (largest longitudinal scale) structure dominates the u'-field and propagates eastward with a phase speed of 15 m/s. In addition, the wavenumber one structure appear in the precipitation field as a modulation of the super clusters.

(3) The vertical structure at the equator is

baroclinic and extends over the whole troposphere.

(4) The latitudinal extent is about the equatorial radius of deformation.

(5) The structure is composed of both equatorial free Kelvin and Rossby wave modes. The northward propagation of the 30–60 day oscillation is not recognized.

The dry experiment verifies that moist processes are essential for maintaining the 30 day oscillation, and hence it is regarded as a wave-CISK mode of its non-linear version. It has a double structure: the existence of small scale (<3000 km) structures (super clusters) and the largest scale (wavenumber one) structure. The appearance of super clusters should be regarded as a new type solution (KR mode) of the equatorial wave-CISK problem, because the slow phase speed (items (1), (2)) and the strong mode coupling (item (5)) are not expected from the linear wave-CISK theory presented so far.

The modulation due to the wavenumber one can be understood as the result of the two dimensional nature of the circulation along the equatorial circumference. The downdraft which compensates the updraft must be located opposite the convectively active region along the equator, and suppress the precipitation there.

The model also shows that a double ITCZ structure appears even when SST minimum does not exist along the equator. The eastward motion of super clusters associated with the 30 day oscillation can be seen with the equatorial belt bounded by the north and south ITCZs.

The 30 day oscillation can be described as a symmetry breaking of the zonally symmetric Hadley circulation. A circulation with zonally symmetric upward motion at the equator and downward motion over the subtropics is not realized, even if the boundary condition is zonally symmetric. The cumulus activity at the equator forms super clusters which move coherently to the east. The 30 day oscillation is intrinsically associated with the equatorial circulation of its idealistic form. The simulation presented here suggests that the 30–60 day oscillation in the actual atmosphere is the result of this intrinsic nature of the equatorial circulation, although it is modified by the effect of

non-zonal distribution of SST and the land-sea contrast of the real surface.

Recently, the 30–60 day oscillation is reported to appear in GCMs with realistic surface boundary conditions (Chiba, 1986; Y. Hayashi and Golder, 1986). The predominant periods simulated in these models differ from one model to another, although they are within the range of 30 to 60 days. An interesting problem placed by these model studies is to search for the conditions additional to our aqua planet model which causes the change in period and structure. Dependency of model oscillations on cumulus parameterization schemes is also a matter of consideration. Through the study of the wave-CISK problem, Lau and Peng (1986) shows the existence of 30 day oscillation by using a simple CISK feedback model. But they do not have a number of super clusters: only wavenumber one structure appears.

Further study is now being made to confirm the discussion presented in section 4 and to reveal the effects of asymmetric surface boundary conditions.

Acknowledgements

List of symbols

u	zonal component of wind
v	meridional component of wind
ω	vertical p-velocity
T	temperature
ϕ	geopotential
Z	geopotential height
θ	latitude
$y \equiv$	$R\theta$
λ	longitude
P	pressure
Ω	Angular frequency of earth's rotation
R	radius of the earth
$\beta \equiv$	$2\Omega/R$
N	buoyancy (Brunt-Vaisala) frequency
c	phase speed of gravity waves
c_0	the phase speed of the "30 day oscillation" (=15 m/s)
$(\bar{\ })$	longitudinal mean of ( )
$(\ )' \equiv (\ ) - (\bar{\ })$	

References

Anderson, D.L.T. and McCreary, J.P., 1985: Slowly propagating disturbances in a coupled ocean-atmosphere model. *J. Atmos. Sci.,* **42**, 615–629.

Chang, C.-P., 1977: Viscous internal gravity waves and low frequency oscillations in the tropics. *J. Atmos. Sci.,* **34**, 901–910.

Charney, J.G., 1971: Tropical cyclogenesis and the formation of the intertropical convergence zone. *Mathematical Problems in Geophysical Fluid Dynamics.* Vol. **13**, Amer. Math. Soc., 255–368.

Chiba, M., 1986: Long-term fluctuation of the tropical atmosphere simulated by the low resolution spectral GCM. *Meteorological Research Report* **86-1**, University of Tokyo, 36–40.

Davies, H.C., 1979: Phase-lagged wave-CISK. *Quart. J. Roy. Met. Soc.,* **105**, 323–353.

Emanuel, K.A., 1983: Elementary aspects of the interaction between cumulus convection and the large-scale environment. in *Mesoscale Meteorology – Theories, Observations and Models* (eds. D.K. Lilly and T. Gal-Chen), Reidel, 551–575.

Gill, A.E., 1980: Some simple solutions for heat-induced tropical circulation. *Quart. J. Roy. Met. Soc.,* **106**, 447–462.

————, 1982: Studies of moisture effects in simple atmospheric models: the stable case. *Geophys. Astrophys. Fluid Dyn.,* **19**, 119–152.

Goswami, B.N. and J. Shukla, 1984: Quasi-periodic oscillations in a symmetric general circulation model. *J. Atmos. Sci.,* **41**, 20–37.

Hayashi, Y., 1970: A theory of large-scale equatorial waves generated by condensation heat and accelerating the zonal wind. *J. Met. Soc. Japan,* **48**, 140–160.

———— and D.G. Golder, 1978: The generation of equatorial transient planetary waves: control experiments with a GFDL general circulation model. *J. Atmos. Sci.,* **35**, 2068–2082.

———— and ————, 1986: Tropical intraseasonal oscillations appearing in a GFDL general circulation model and FGGE data. Part I: Phase propagation. *J. Atmos. Sci.* (submitted).

Heckley, W.A. and A.E. Gill, 1984: Some simple analytical solutions to the problem of forced equatorial long waves. *Quart. J. Roy. Met. Soc.,* **110**, 203–

217.

Kanamitsu, M., K. Tada, T. Kudo, N. Sato and S. Isa, 1983: Description of the JMA operational spectral model. *J. Met. Soc. Japan,* **61**, 812–828.

Knutson, T.R., K.M. Weickmann and J.E. Kutzbach, 1986: Global scale intraseasonal oscillations of outgoing longwave radiation and 250 mb zonal wind during northern hemispheric summer. *Mon. Wea. Rev.,* **114**, 605–623.

Kuo, H.L., 1974: Further studies of the influence of cumulus convection on large-scale flow. *J. Atmos. Sci.,* **31**, 1232–1240.

Lau, K.-M. and P.H. Chan, 1983a: Short-term climate variability and atmospheric teleconnections from satellite-observed outgoing longwave radiation. Part I: Simultaneous relationships. *J. Atmos. Sci.,* **40**, 2735–2750.

―――― and ――――, 1983b: Short-term climate variability and atmospheric teleconnections from satellite-observed outgoing longwave radiation, Part II: Lagged correlations. *J. Atmos. Sci.,* **40**, 2751–2767.

―――― and ――――, 1985: Aspects of the 40–50 day oscillation during the northern winter as inferred from outgoing longwave radiation. *Mon. Wea. Rev.,* **113**, 1889–1909.

―――― and L. Peng, 1986: Origin of low frequency (intraseasonal) oscillations in the tropical atmosphere. Part I: The basic theory *(personal communication).*

Lindzen, R.S., 1974: Wave-CISK in the tropics. *J. Atmos. Sci.,* **31**, 156–179.

Madden, R.A. and P.R. Julian, 1972: Description of global-scale circulation cells in the tropics with a 40–50 day period. *J. Atmos. Sci.,* **29**, 1109–1123.

Matsuno, T., 1966: Quasi-geostrophic motions in the equatorial area. *J. Met. Soc. Japan,* **44**, 25–43.

Maruyama, T., 1982: Upper tropospheric zonal wind oscillation with a 30–50 day period over the equatorial western Pacific observed in cloud movement vectors. *J. Met. Soc. Japan,* **60**, 172–182.

Monthly Report of Meteorological Satellite Center. Meteorological Satellite Center, Japan Met. Agency.

Murakami, M., 1972: Intermediate-scale disturbances appearing in the ITC zone in the tropical Western Pacific. *J. Met. Soc. Japan,* **50**, 454–464.

――――, 1984: Analysis of the deep convective activity over the western Pacific and southeast Asia. Part II: Seasonal and intraseasonal variations during northern summer. *J. Met. Soc. Japan,* **62**, 88–108.

――――, 1985: On the 30–50 day period variations of the atmospheric circulation. *Tenki,* **32**, 479–482 (in Japanese).

Murakami, T., T. Nakazawa and J. He, 1984: On the 40–50 day oscillations during the 1979 northern hemisphere summer, Part I: Phase propagation. *J. Met. Soc. Japan,* **62**, 440–468.

―――― and ――――, 1985: Tropical 45 day oscillation during the 1979 northern hemispheric

summer. *J. Atmos. Sci.,* **42**, 1107–1122.

――――, L.-X. Chen, A. Xie and M.L. Shrestha, 1986: Eastward propagation of 30–60 day perturbation as revealed from outgoing longwave radiation data. *J. Atmos. Sci.,* **42**, 961–971.

Nakazawa, T., 1986: Mean features of 30–60 day variations as infered from 8-year OLR data. *J. Meteor. Soc. Japan* (to appear).

Parker, D.E., 1973: Equatorial Kelvin waves at 100 millibars. *Quart. J.R. Met. Soc.,* **99**, 116–129.

Philander, S.G.H., T. Yamagata and R.C. Pacanowski, 1984: Unstable air-sea interactions in the tropics. *J. Atmos. Sci.,* **41**, 604–613.

Pike, A.C., 1971: Intertropical convergence zone studied with an interacting atmosphere and ocean model. *Mon. Wea. Rev.,* **99**, 469–477.

Quah, L.C., 1984: On the 30–50 day tropospheric oscillation during the northern winter. *J. Met. Soc. Japan,* **62**, 261–272.

Sardeshmukh, P.D. and B.J. Hoskins, 1985: Vorticity balances in the tropics during the 1982–83 El Niño–Southern Oscillation event. *Quart. J. Roy. Met. Soc.,* **111**, 261–278.

Sumi, A. and M. Kanamitsu, 1984: A study of systematic errors in a numerical weather prediction model. Part I: General aspects of the systematic errors and their relation with the transient eddies. *J. Met. Soc. Japan,* **62**, 234–250.

Webster, P.J., 1983: Mechanisms of monsoon low-frequency variability: Surface hydrological effects. *J. Atmos. Sci.,* **40**, 2110–2124.

Weickmann, K.M., G.R. Lussky and J.E. Kutzbach, 1985: Intraseasonal (30–60 days) fluctuations of outgoing long wave radiation and 250 mb streamfunction during northern winter. *Mon. Wea. Rev.,* **113**, 941–961.

Wallace, J.M. and V.E. Kousky, 1968: Observational evidence of Kelvin waves in the tropical stratosphere. *J. Atmos. Sci.,* **25**, 900–907.

Yamagata, T. and Y. Hayashi, 1984: A simple diagnostic model for the 30–50 day oscillation in the tropics. *J. Met. Soc. Japan,* **62**, 709–717.

――――, 1985: Stability of a simple air-sea coupled model in the tropics. in *Coupled ocean-atmosphere models* (ed. J.C.J. Nihoul), Elsevier.

Yamasaki, M., 1969: Large-scale disturbances in a conditionally unstable atmosphere in low latitudes. *Papers in Met. and Geophys.,* **20**, 289–336.

Yanai, M., S. Esbensen and J.-H. Chu, 1973: Determination of bulk properties of tropical cloud clusters from large-scale heat and moisture budgets. *J. Atmos. Sci.,* **30**, 611–627.

Yasunari, T., 1980: A quasi-stationary appearance of 30 to 40 day period in the cloudiness fluctuations during the summer monsoon over India. *J. Met. Soc. Japan,* **58**, 225–229.

――――, 1981: Structure of an Indian summer monsoon system with around 40-day period. *J. Met. Soc. Japan,* **59**, 336–354.

『水惑星』モデルでシミュレートされた30－40日周期振動

林　祥介・住　明正

東京大学理学部地球物理学教室

　積雲対流活動の集団的運動（いわゆる wave-CISK）に起因する長周期（30－40日程度）変動の可能性を議論するために，南北対称・東西一様なる仮想的海洋におおわれた『水惑星』上での大気のふるまいを大気大循環モデルを用いた数値実験により調べた。

　90日間の積分結果は対流活動の集団的運動が自発的に出現することを示した。それにともなう東西循環は，現実大気で知られている30－60日周期振動に類似した特徴を持つ。この循環（『30日周期振動』）は，赤道変形半径に特徴づけられる『スーパークラスター』とその変調として現れる『波数1』とからなる空間的二重構造を持っており，全体としてゆっくり（15m/s）東向きに伝わる。

　モデルはまた，二重赤道収束帯をも再現した。赤道上に低海水面温度域が存在しなくとも赤道収束帯は赤道をまたいで南北二本存在する。この両収束帯にかこまれた領域では積雲活動は，スーパークラスターとして組織されるが，一方その外側では熱帯低気圧（台風）として組織される。

　湿潤過程の除去は30日周期振動の赤道ケルビン波・ロスビー波への崩壊をもたらした。このことは30日周期振動の構造が，赤道波間の強いモード結合により維持されていることを示す。対流活動の集団的運動のこれらの特徴（遅い位相速度・モード結合・空間的二重構造）はこれまでの線形 wave-CISK 理論のケルビン波モードでは説明できない。『30日周期振動』は赤道 wave-CISK 問題に対する新種の解とみなすことができよう。